Cent. Eur. J. Phys.
DOI: 10.2478/s11534-010-0111-z

VERSITA

Central European Journal of **Physics**

Modeling of flow and mass transport in granular porous media

Research Article

Frank A. Coutelieris*

Department of Environmental and Natural Resources Management, University of Ioannina, Seferi 2, 30100, Agrinio, Greece

Received 3 July 2010; accepted 25 October 2010

Abstract: The scope of this work is to estimate the effective mass-transfer coefficient in a two-phase system of oil and water fluid droplets, both being in a porous medium. To this end, a tracer is advected from the flowing aqueous phase to the immobile non-aqueous one. Partitioning at the fluid-fluid interface and surface diffusion are also taken into account. By using spatial/volume-averaging techniques, the appropriately simplified boundary-value problems are described and numerically solved for the flow velocity field and for the transport problem. The problem was found to be controlled by the Peclet number of the flowing phase, the dimensionless parameter Λ, containing both diffusion and partition in the two phases, as well as the geometrical properties of the porous structure. It is also verified that the usually involved unit cell-configurations underestimate the mass transport to the immobile phase.

PACS (2008): 02.60.Cb, 02.60.Nm, 82.20.-w, 82.30.-b

Keywords: convection • diffusion • mass transfer • multiphase flow • porous media

1. Introduction

Mathematical modeling of multiphase transport processes in porous media is a powerful tool employed whenever experimentation is either expensive or difficult due to the nature of the process. A realistic description of the porous structure significantly increases the complexity of the mathematics involved, due to the coupling between the physicochemical mechanisms and the geometrical complexity of the porous medium. Modeling becomes more difficult when moving from the pore level to the field level, because different length scales result in complicated descriptions of the physics of the problem and therefore requires massive computational power.

The major issue of typical macroscopic modeling for such cases can be identified at the a-priori definition of the mass transport coefficient and the dispersion tensor, which are necessary for the solution of these equations although they are macroscopic quantities normally derived from the solution of these equations. So far, mainly empirical or semi-empirical correlations of Sherwood with Peclet number (which include these parameters) have been proposed based on experimental measurements of specific systems [1]. On the other hand, the generalized treatment of such a problem corresponds to theoretical estimations of these quantities where the volume averaging concept is

*E-mail: fkoutel@cc.uoi.gr

a frequently employed tool for large scale modeling of processes that take place in porous media, eliminating the influence of porous structure (geometry) on transport results [2–5]. Starting from transport equations at the micro-scale (pore) level, the spatial averaging theorem is applied along with the proper assumptions, leading to the estimation of macroscopic quantities such as mass transfer coefficient and dispersion tensor [6, 7].

Of great importance for industrial and technological applications are these physicochemical processes where an aqueous phase coexists and/or interacts with a non-aqueous liquid one within a porous medium. At most of the models used for describing such processes, mass exchange between the two liquid phases has been considered at some extent and modeled under a variety of different approaches, such as phenomenological approximations that make use of an additional term, which is equivalent to the rate of mass transfer between the two phases (see, for example [8]) or sufficiently fast diffusion in the non-aqueous phase (see, for example [9]). Mass exchange between the two phases has also been modelled by considering either a controlling diffusive process, which is macroscopically described by a first-order kinetic, or an advection process in the less permeable zone [10–15]. Obviously, these assumptions are a rough representation of the real world, thus a more complicated model has recently been proposed, which takes into account interfacial diffusion in both phases and partitioning phenomena [16]. To further simplify the mathematical modeling and to eliminate the simulation effort, the majority of the above-mentioned cases/models were applied in quite simplistic domains (unit cell, etc.), since the interest was on the interfacial mass exchange rather than on representing the medium as realistically as was possible.

In the present work, we apply the stylish approach, that is typically used for the mass interfacial exchange [16], to 3-D porous structures representing granular media. In that respect, the aim of this work is to estimate the mass transport coefficient and to investigate how different structural and physicochemical parameters affect it. In order to demonstrate the validity of this approach, a comparison with other existing theoretical results is attempted.

2. Mathematical formulation

The area of interest is a multi-phase domain consisting of a flowing aqueous phase (β-phase), an immobile non-aqueous liquid phase (γ-phase), and a solid phase (σ-phase). A partitioning tracer is advected by the flowing β-phase and undergoes partitioning in the immobile phase into which it is diffusing. It is also assumed that the solid phase is physico-chemically neutral, i.e. the tracer is neither adsorbed nor reacts with the σ-phase. The governing processes are diffusion and advection in the β-phase, and diffusion in the γ-phase. The mass exchange at the $\beta\gamma$ interface is characterized by the diffusion and partitioning properties of the tracer.

The pore-level transport of the tracer in the β-phase is described by the diffusion-advection equation

$$\frac{\partial C_\beta}{\partial t} + \nabla \cdot (\mathbf{v} C_\beta) = D_\beta \nabla^2 C_\beta, \tag{1}$$

where C_β is concentration, t is time, $\mathbf{v}$ is the fluid velocity and D_β is the diffusivity in the β-phase. Since the γ-phase is assumed immobile, the diffusion equation describes the transport of tracer in that phase

$$\frac{\partial C_\gamma}{\partial t} = D_\gamma \nabla^2 C_\gamma, \tag{2}$$

where C_γ and D_γ are concentration and diffusivity in the γ-phase, respectively. Zero-flux boundary conditions apply on the solid-liquid interfaces

$$\mathbf{n}_{\beta\sigma} \cdot \nabla C_\beta = 0 \text{ at } A_{\beta\sigma}, \tag{3a}$$

$$\mathbf{n}_{\gamma\sigma} \cdot \nabla C_\gamma = 0 \text{ at } A_{\gamma\sigma}, \tag{3b}$$

as the transported species does not absorb or react at the solid. At the interface $A_{\beta\gamma}$ between the trapped and flowing phases, the conditions for partition equilibrium and flux continuity at the interface are applied [16]

$$C_\gamma = K C_\beta, \tag{4a}$$

$$D_\beta \mathbf{n}_{\beta\gamma} \cdot \nabla C_\beta = D_\gamma \mathbf{n}_{\beta\gamma} \cdot \nabla C_\gamma, \tag{4b}$$

where K is the partitioning coefficient.

Following the volume-averaging procedure, which is presented briefly in Table 1 and in detail elsewhere [1, 16], the above problem can be transformed to the following dimensionless system

$$Pe_\beta u \cdot \nabla \phi_\beta = \nabla^2 \phi_\beta - \Lambda \text{ in the } \beta\text{-phase}, \tag{5}$$

$$\mathbf{n}_{\beta\sigma} \cdot \nabla \phi_\beta = 0 \text{ at } A_{\beta\sigma}, \tag{6}$$

$$0 = \nabla^2 \phi_\gamma + 1 \text{ in the } \gamma\text{-phase}, \tag{7}$$

$$\mathbf{n}_{\gamma\sigma} \cdot \nabla \phi_\gamma = 0 \text{ at } A_{\gamma\sigma}, \tag{8a}$$

$$\phi_\beta = \phi_\gamma \text{ at } A_{\beta\gamma}, \tag{8b}$$

$$\langle \phi_\gamma \rangle = 0, \tag{8c}$$

where

$$Pe_\beta = \frac{\langle \mathbf{v} \rangle^\beta l_\beta}{D_\beta}$$

Table 1. The spatial averaging technique (as in [16]).

	Differential equations with Boundary Conditions and Compatibility Conditions	Mass transfer coefficient
Pore level formulation	$\frac{\partial C_\beta}{\partial t} + \nabla \cdot \left(\mathbf{v} C_\beta\right) = D_\beta \nabla^2 C_\beta$	
	$\frac{\partial C_\gamma}{\partial t} = D_\gamma \nabla^2 C_\gamma$	
	$\mathbf{n}_{\beta\sigma} \cdot \nabla C_\beta = 0$ at $A_{\beta\sigma}$	
	$\mathbf{n}_{\gamma\sigma} \cdot \nabla C_\gamma = 0$ at $A_{\gamma\sigma}$	
	$C_\gamma = K C_\beta$ at $A_{\beta\gamma}$	
	$D_\beta \mathbf{n}_{\beta\gamma} \cdot \nabla C_\beta = D_\gamma \mathbf{n}_{\beta\gamma} \cdot \nabla C_\gamma$ at $A_{\beta\gamma}$	
Decomposition	$\mathbf{v}_\beta \cdot \nabla s_\beta = D_\beta \nabla^2 s_\beta - \varepsilon_\beta^{-1} \alpha$	$\alpha = \frac{D_\beta}{V} \int\limits_{A_{\beta\gamma}} \mathbf{n}_{\beta\gamma} \cdot \nabla s_\beta dA$
$C_\beta = \langle C_\beta \rangle^\beta + C'_\beta$	$D_\gamma \nabla^2 s_\gamma = -\varepsilon_\gamma^{-1} \alpha$	
$C_\gamma = \langle C_\gamma \rangle^\gamma + C'_\gamma$	$s_\beta = 1 + \frac{s_\gamma}{K}$ at $A_{\beta\gamma}$	
$\mathbf{v}_\beta = \langle \mathbf{v}_\beta \rangle^\beta + \mathbf{v}'_\beta$	$D_\beta \mathbf{n}_{\beta\gamma} \cdot \nabla \mathrm{s}_\beta = D_\gamma \mathbf{n}_{\beta\gamma} \cdot \nabla \mathrm{s}_\gamma$ at $A_{\beta\gamma}$	
	$\mathbf{n}_{\beta\sigma} \cdot \nabla s_\beta = 0$ at $A_{\beta\sigma}$	
	$\mathbf{n}_{\gamma\sigma} \cdot \nabla s_\gamma = 0$ at $A_{\gamma\sigma}$	
	$\langle s_\beta \rangle = 0$	
	$\langle s_\gamma \rangle = 0$	
Transformation	$Pe_\beta v \cdot \nabla \zeta_\beta = \nabla^2 \zeta_\beta - \varepsilon_\beta^{-1}$	$\alpha^* = -\frac{\varepsilon_\beta}{\langle \zeta_\beta \rangle}$
$s_\beta = 1 + \alpha^* \zeta_\beta$	$0 = \delta \nabla^2 \zeta_\gamma + \varepsilon_\gamma^{-1}$	
$s_\gamma = \alpha^* \zeta_\gamma$	$\mathbf{n}_{\beta\sigma} \cdot \nabla \zeta_\beta = 0$ at $A_{\beta\sigma}$	
	$\mathbf{n}_{\gamma\sigma} \cdot \nabla \zeta_\gamma = 0$ at $A_{\gamma\sigma}$	
	$\zeta_\beta = \frac{1}{K} \zeta_\gamma$ at $\mathrm{A}_{\beta\gamma}$	
	$\langle \zeta_\gamma \rangle = 0$	
Substitution	$Pe_\beta u \cdot \nabla \phi_\beta = \nabla^2 \phi_\beta - \Lambda$	$\alpha^* = -\frac{\delta K \varepsilon_\beta \varepsilon_\gamma}{\langle \phi_\beta \rangle}$
$\phi_\beta = \delta K \varepsilon_\gamma \zeta_\beta$	$0 = \nabla^2 \phi_\gamma + 1$	
$\phi_\gamma = \delta \varepsilon_\gamma \zeta_\gamma$	$\mathbf{n}_{\beta\sigma} \cdot \nabla \phi_\beta = 0$ at $A_{\beta\sigma}$	
	$\mathbf{n}_{\gamma\sigma} \cdot \nabla \phi_\gamma = 0$ at $A_{\gamma\sigma}$	
	$\phi_\beta = \phi_\gamma$ at $A_{\beta\gamma}$	
	$\langle \phi_\gamma \rangle = 0$	

is the Peclet number defined in the β-phase by using a length l_β characteristic for this phase, u is the dimensionless velocity vector, ϕ_β, ϕ_γ are scalar variables used for the decomposition (see [16]) and

$$\Lambda = \frac{\delta K \varepsilon_\gamma}{\varepsilon_\beta},$$

with ε_β, ε_γ the volume fraction of the β- and γ-phase, respectively, and

$$\delta = \frac{D_\gamma}{D_\beta}.$$

In accordance with the above approach, the dimensionless mass-transfer coefficient is simply [16]

$$\alpha^* = -\frac{\delta K \varepsilon_\beta \varepsilon_\gamma}{\langle \phi_\beta \rangle}. \tag{9}$$

Brackets denote averages, such that for any function y_i associated with the i-phase (either β or γ), the superficial volume average is defined as

$$\langle y_i \rangle = \frac{1}{V} \int_{V_i} y_i dV \tag{10}$$

and the interstitial volume average as

$$\langle y_i \rangle^i = \frac{1}{V_i} \int_{V_i} y_i dV. \tag{11}$$

By V we denote the total volume of the porous material, with V_β and V_γ being the volumes of aqueous and non-aqueous phases, respectively.

3. Simulations

3.1. Geometry

To define a realistic domain for the solution of the flow and transport problems, a granular porous medium was constructed in the form of a spherical particle assemblage. Specifically, the representation of the domains under consideration has been achieved by the random deposition of rigid spheres of a given radius in a box of specified dimensions, while the spherical droplets are again randomly positioned in the remaining void space so as to assure both the overall porosity of the medium and the volume fraction of the non-aqueous phase. A sample medium with overall porosity of 0.72 and $\varepsilon_\beta = 0.12$ is graphically presented in Fig. 1.

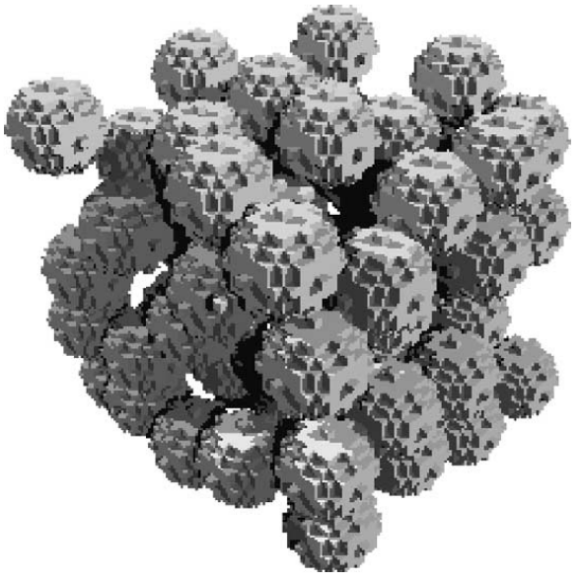

Figure 1. Schematical representation of 3-D granular medium.

3.2. Flow-field

The velocity field was computed numerically by solving the Stokes equations

$$\nabla p = \mu \nabla^2 \mathbf{v}, \tag{12a}$$

$$\nabla \cdot \mathbf{v} = 0, \tag{12b}$$

$$\mathbf{v} = \mathbf{0} \text{ at } A_{\beta\sigma}, \tag{12c}$$

where $\mathbf{v}$, p, and μ are the velocity vector, the pressure field and the fluid viscosity, respectively. Obviously, the velocity $\mathbf{v}$ at any point has been afterwards normalized with the characteristic velocity magnitude to obtain the dimensionless velocity u used in Eq. (5). The procedure for solving the 3D Stokes flow problem involves discretization in terms of cubic elements and is described as follows [17]: At the pore level, a staggered marker-and-cell (MAC) mesh is used, with the pressure defined at the center of the cell and the velocity components defined along the corresponding face boundaries. The resulting linear system of equations is solved by a successive over-relaxation (SOR) method. An initial guess for p is determined through the solution of a Laplace equation. Next, the velocity vector $\mathbf{v}$ is calculated from the corresponding momentum balance and the continuity equation $\nabla \cdot \mathbf{v} = 0$. The pressure is corrected through an artificial compressibility equation of the form

$$\frac{dp}{dt} = \nabla \cdot \mathbf{v}. \tag{13}$$

The above steps are repeated until convergence is reached. This numerical scheme for the determination of the velocity field has been widely validated in terms of both the velocity field and the corresponding permeability [18].

Fig. 2a, 2b and 2c show the results of the pressure-field, the velocity and the stream function for a typical porous medium of $\varepsilon = 0.72$. A randomly selected 2-D cut of the medium is considered in order for the results to be clearly visualized. The boundary condition at the closed walls is no-slip, at the left boundary we impose an inflow and at the right boundary an outflow condition. Small vortices and recirculating flow are produced in the medium, depending on the pore size, while smoother profiles are obtained at the inlet and outlet. The velocity gradient from top to bottom at the inlet surface is because the inflow condition assures constant molar flux instead of plug-type velocity vector. Finally, it is interesting to observe that the faster flow paths are generated by the porous structure and appear wherever the pore diameters are quite small.

3.3. Algorithm

To adequately simulate the above-described problem, an algorithmic procedure has been developed as follows:

- Solve the flow problem at the pore level and calculate interstitial and superficial velocity fields.
- Formulate the mass transport problem at the pore level.
- Decompose the local velocities and concentrations in terms of interstitial averages and fluctuations.
- Describe the concentration fluctuations in terms of linear combinations of interstitial averaged concentrations and their gradients.
- Solve $\tau\eta\epsilon$ closure problems.
- Integrate the resulting quantities to calculate macroscopic coefficients.

3.4. Numerical scheme

The simulated geometry was discretized in space by a structure grid consisting of more than 1 million cells, since the size of the digitized domains was $102 \times 102 \times 102$ grid points for all the simulations. The grid spacing is chosen to be non-uniform because it has been proven that appropriately non-uniform discretization performs better than the equal-spaced one [19]. For the numerical solution of the closure boundary value problems, a non-uniform finite difference scheme with upwinding was used, with the

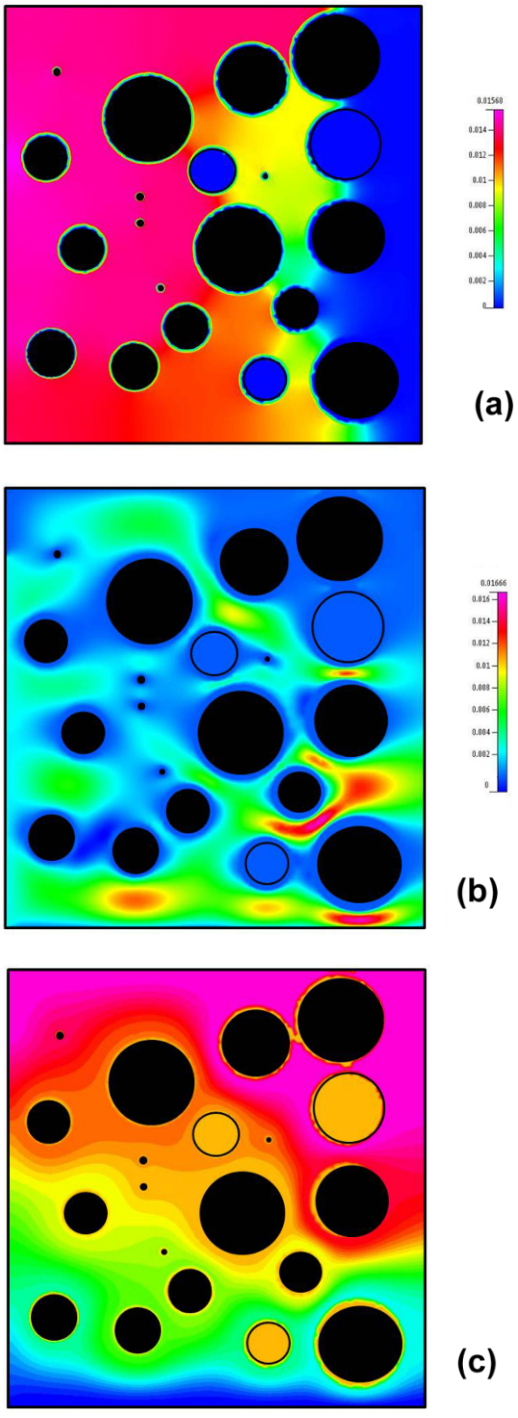

Figure 2. Snapshot of the pressure field (a), velocity (b) and stream lines (c) simulations through the representative porous medium with the flow direction from left to right. Black bodies correspond to solid phase and transparent ones to the γ-phase.

resulting linear systems of equations solved using successive over-relaxation (SOR) [20]. Residual values lower than 10^{-4} were achieved for all the unknown quantities and the computational needs were satisfied by an Intel Pentium 3.2 GHz computer. The steady-state condition was assumed to be achieved whenever the relative difference for all the results of two sequential time-steps was lower than 0.0001%. Under these conditions, the necessary time for each run was approximately about half a day (including the solution for the flow-field). Several runs were carried out to perform the following parametric analysis for the above described model.

4. Results and discussion

At this point, it is important to stress once more the significance of parameter Λ because it corresponds to a significant reduction of the parameters involved in the description of the process. For example, this concept provides assurance that the diffusivity ratio has practically the same effect with the partitioning coefficient, since these parameters are related through the Λ expression. Similar conclusions can be drawn for the ratio of the phase porosities, as well. Following the above, the effect of the dimensionless parameter Λ on the dimensionless mass transfer coefficient is shown in Fig. 3, for two different values of the Peclet number. It is clearly shown that the mass transport coefficient rapidly increases with Λ at low Λ values, and reaches a constant value at high Λ. The porous geometry positively affects the value of the mass transfer coefficient: the case when a realistic 3-D porous geometry is considered yields mass transfer coefficients always larger than those corresponding to unit-cell approximations. This is a result of the higher surface area per unit volume available in the case of 3-D structures with a lot of droplets in comparison to those for otherwise the same volumetric fractions. The coefficient is independent of the Peclet number for low Λ values; the same is also predicted by other theoretical works [16, 21]. On the other hand, the higher the Peclet value, the larger the amount of mass exchange at the fluid-fluid interface, as the mass transport coefficient indicates. This is because strong convective regimes in porous structures usually eliminate the possibility for the tracer to escape from the bubbles' surface. This behavior is further observed in Fig. 4, where the effect of the pore-scale Peclet number on the dimensionless mass transfer coefficient is shown. As before, the mass-transfer coefficient is higher in the case when the representation of porous medium is more realistic. Finally, the effect of the geometry on the process is presented in Fig. 5, where the mass-transfer coefficient is depicted as a function of the

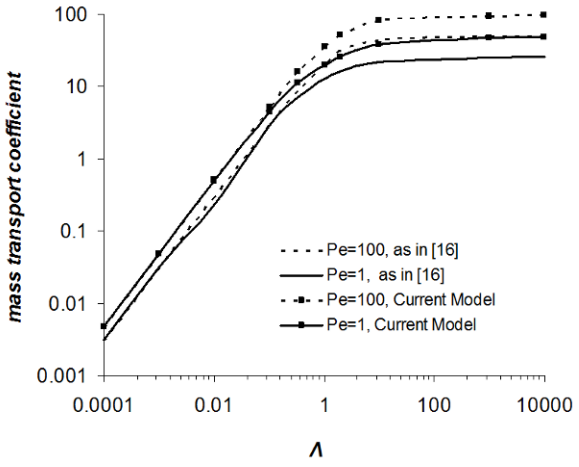

Figure 3. The mass-transfer coefficient as a function of Λ.

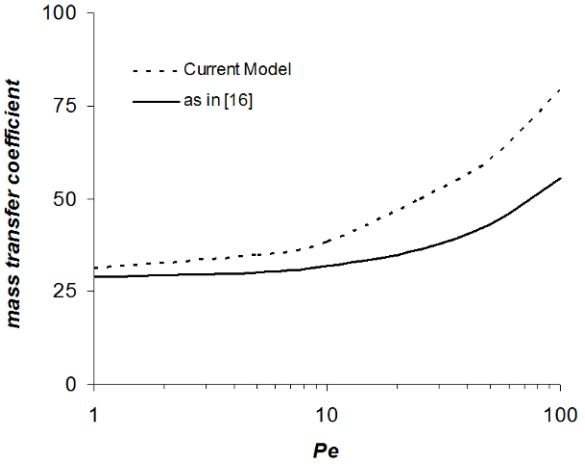

Figure 4. The effect of the Peclet number on the mass-transfer coefficient for a medium of $\varepsilon_\beta = 0.39$ and $\varepsilon_\gamma = 0.04$.

volume fraction of γ-phase. It is important to note that in these simulations, the dry porosity remains constant and equal to 0.43, while ε_γ varied between 0.4 and 0.12, thus ε_β varied in the interval 0.39-0.31, respectively. It can be observed that as ε_γ decreases so does the mass transfer coefficient, in accordance with existing results presented elsewhere [8, 11, 16]. The discrete points in this figure correspond to predictions by using the unit cell approach [16], where again, the mass transport coefficient has been underestimated.

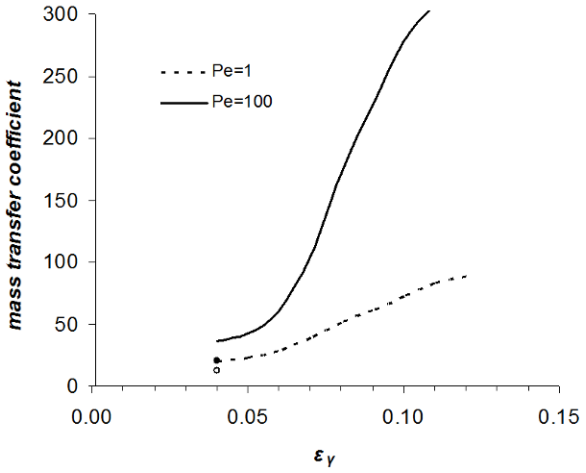

Figure 5. The effect of the volume fraction of γ-phase on the mass-transfer coefficient. Dry porosity is 0.43.

5. Conclusions

In this paper, the effective mass-transfer coefficient between two fluid phases in a porous medium is derived. One of the phases is assumed to be flowing and the other as immobile while a passive tracer is advected by the flowing phase, undergoes partitioning at the fluid-fluid interface and diffuses in the immobile phase. By using the volume-averaging method, the relative closure problems have been defined and applied in a 3-D artificial representation of a typical granular porous medium. The numerical solution within this domain allows for the calculation of the effective mass-transfer coefficient. The problem was shown to be controlled by the Peclet number of the flowing phase and the dimensionless parameter Λ, including the diffusion and the geometrical properties of the porous medium. By comparing the current results with other theoretical estimations, it is found that the unit-cell geometry underestimates the mass transport coefficient because of the lower surface area considered.

Acknowledgments

The author would like to thank Dr. A. Stubos and Dr. M. Kainourgiakis from National Centre for Scientific Research "Demokritos", Greece, for their useful discussions on the topic.

References

[1] M. Quintard, S. Whitaker, Adv. Water Resour. 17, 221 (1994)
[2] R.G. Carbonell, S. Whitaker, In: J. Bear, M.Y. Carpacioglu (Eds.), Fundamentals of Transport Phenomena in Porous Media (Martinus Nijhof Publ., Dordrecht, Netherlands, 1984) 121
[3] F. Zanotti, R.G. Carbonell, Chem. Eng. Sci. 39, 263 (1984)
[4] F. Zanotti, R.G. Carbonell, Chem. Eng. Sci. 39, 279 (1984)
[5] S. Whitaker, AIChE J. 13, 420 (1967)
[6] M. Quintard, S. Whitaker, Advances in Heat Transfer 23, 369 (1993)
[7] M. Quintard, S. Whitaker, Chem. Eng. Sci. 48, 2537 (1993)
[8] A.C. Lam, R.S. Schechter, W.H. Wade, Soc. Petrol. Eng. J. 23, 781 (1983)
[9] H. Gvirtzam, N. Paldor, M. Magaritz, Y. Bachmat, Water Resour. Res. 24, 1638 (1988)
[10] A. Ahmadi, M. Quintard, S. Whitaker, Adv. Water Resour. 22, 59 (1998)
[11] J.-P. Gwo, R. O'Brien, P.M. Jardine, J. Hydrol. 208, 204 (1998)
[12] T. Vogel, H. Gerke, R. Zhang, M.V. Genuchten, J. Hydrol. 238, 78 (2000)
[13] G. Dagan, S. Lessoff, Water Resour. Res. 37, 465 (2001)
[14] S. Lessoff, G. Dagan, Water Resour. Res. 37, 473 (2001)
[15] P.E. Kechagia, I.N. Tsimpanogiannis, Y.C. Yortsos, P.C. Lichtner, Chem. Eng. Sci. 57, 2565 (2002)
[16] F.A. Coutelieris, M.E. Kainourgiakis, A.K. Stubos, E.S. Kikkinides, Y.C. Yortsos, Chem. Eng. Sci. 61, 4650 (2006)
[17] P.M. Adler, C.J. Jacquin, J.A. Quiblier, Int. J. Multiphas. Flow 16, 691 (1990)
[18] E.S. Kikkinides, V.N. Burganos, Phys. Rev. E. 62, 6906 (2000)
[19] L.M. Sun, M.D. Levan, Chem. Eng. Sci. 50, 163 (1995)
[20] W.H. Press, B.P. Flanner, S.A. Teukolsky, W.T. Vetterlling, Numerical recipes (Cambridge University Press, Cambridge, UK, 1986)
[21] A. Ahmadi, A. Aigueperse, M. Quintard, Adv. Water Resour. 24, 423 (2001)